Extended Hückel Molecular Orbital Study of the Effects of Edge-bridging Hydrogen Atoms on the Lengths of Boron–Boron and Metal–Metal Bonds in Cluster Compounds, and the Crystal Structure of Benzyltrimethylammonium Octahydrotriborate(1 −)†

Gary F. Mitchell and Alan J. Welch*
Department of Chemistry, University of Edinburgh, Edinburgh EH9 3JJ

The origin of the lengthening of B–B and M–M (M = transition metal) connectivities in borane and transition-metal cluster compounds as a consequence of edge H-bridging is traced, *via* EHMO–FMO calculations on $[B_{11}H_{13}]^{2-}$, $[Os_4H_2(CO)_{12}]^{2-}$, $[Re_3H(CO)_{12}]^{2-}$ and $[Re_3H_2(CO)_{12}]^-$, to asymmetry in the occupation of formerly degenerate orbitals of the cluster upon protonation. The unusual relative shortening of the bridged B–B connectivities in $[B_3H_8]^-$ is confirmed by an accurate, low-temperature crystallographic study of the ion as its $[PhCH_2NMe_3]^+$ salt. Crystals are monoclinic, space group $P2_1/c$ with four ion pairs in a cell of dimensions a = 11.225(4), b = 9.483(3), c = 13.218(4) Å, β = 111.70(3)°; R = 0.0569 for 2 903 data measured at 185 K. EHMO–FMO calculations show that the B–B edge shortening in $[B_3H_8]^-$ is strongly correlated with the asymmetric nature of the H-bridges, and that these two distortions are mutually self-regulating. A combined EHMO–FMO and MNDO study of the B–B edge protonation of 1,6-$C_2B_4H_6$ suggests that the edge shortening which has previously been predicted may be incorrect.

It is widely held that the effect of a hydrogen bridge is to cause lengthening (by *ca.* 0.1—0.15 Å) of a B–B or M–M (M = transition metal) connectivity in a polyhedral borane or transition-metal cluster compound.[1–3,‡] This principle is now so well established that it has become fairly standard practice in *X*-ray crystallographic studies of such species to make use of the lengthening to assume H-atom positions when they are not directly located.[5]

Surprisingly, no theoretical explanation of the cause of this lengthening has, to our knowledge, ever been offered. One simplistic approach would be to invoke polarisation of the electron density in a three-centre B–H–B or M–H–M bond towards the H atom, but this explanation fails to account for the known structures of apparent anomalies such as $[B_3H_8]^-$,[6] in which H-bridging is associated with *shortening* of the appropriate bond.

The structure of $[B_3H_8]^-$ is particularly interesting in that, in addition to the μ-H atoms residing on short B–B connectivities, the B–μ-H bond lengths are unusually asymmetric. Although both these features of the structure have been reproduced by high-level geometry-optimised molecular orbital (m.o.) calculations,[7] no rationalisation has been advanced.

In this paper we use the results of extended Hückel molecular orbital (EHMO) calculations to identify the cause of the general lengthening of B–B and M–M connectivities in clusters as a consequence of H-bridging. We also identify the asymmetry of the H-bridges in $[B_3H_8]^-$ as the origin of the unusual shortening of the bridged B–B bonds. Moreover, since the structure of $[B_3H_8]^-$ was determined many years ago[6] we have confirmed the important features of the structure by an accurate, low-temperature crystallographic study of the ion as a different salt. Finally, we have critically reinvestigated [*via* EHMO and modified neglect of diatomic overlap (MNDO) calculations] the B–B edge protonation of *closo*-1,6-$C_2B_4H_6$. Here an earlier MNDO study[8] had predicted shortening of the protonated edge, and this unusual result had been explained by polarisation arguments.

Experimental

Syntheses.—A number of salts of $[B_3H_8]^-$ were prepared by the general method of reaction of $Tl[B_3H_8]$[9] with the chloride or bromide of an appropriate cation. In a typical reaction $[PhCH_2NMe_3]Br$ (0.6334 g, 2.75 mmol) in $MeOH–H_2O$ (3:1, 10 cm³) was added with stirring to $Tl[B_3H_8]$ (0.6739 g, 2.75 mmol) in the same solvent mixture (10 cm³). The precipitate of TlBr was filtered off and the filtrate evaporated *in vacuo* to afford $[PhCH_2NMe_3][B_3H_8]$ (**1**) as a colourless solid in almost quantitative yield (Found: C, 62.8; H, 12.65; N, 7.30. $C_{10}H_{24}B_3N$ requires C, 63.0; H, 12.7; N, 7.35%).

The compounds $[NEt_4][B_3H_8]$ (**2**), $[NPr_4][B_3H_8]$ (**3**), and $[N(PPh_3)_2][B_3H_8]$ (**4**), were prepared similarly.

X-Ray Crystallography.—Numerous crystallisations of (**1**)—(**4**) and of commercially-supplied $[NMe_4][B_3H_8]$ (**5**) were attempted. Although diffraction data were collected from the best samples of all species, those from (**2**)—(**5**) could not be either solved or satisfactorily refined because of poor crystal quality and/or disorder that could not be adequately modelled. Preliminary data for these salts are given in Table 1.

In contrast, (**1**) forms as diffraction-quality crystals by slow evaporation of a CH_2Cl_2 solution. A single crystal (0.4 × 0.4 × 0.3 mm) was mounted on a glass fibre with low-temperature epoxy-resin adhesive and, after preliminary Weissenberg photography, slowly cooled to 185 K on an Enraf-Nonius CAD4 diffractometer fitted with a ULT-1 attachment.

Crystal data. $C_{10}H_{24}B_3N$, M = 190.7, monoclinic, a = 11.225(4), b = 9.483(3), c = 13.218(4) Å, β = 111.70(3)°, U = 1 307.4 Å³ by the least-squares refinement of 25 centred reflections, 14 < θ < 15°, λ = 0.710 69 Å, T = 185 K, space

† *Supplementary data available* (No. SUP 56667, 7 pp.): atomic co-ordinates used in EHMO calculations, MNDO-optimised co-ordinates, unit-cell packing diagram. See Instructions for Authors, *J. Chem. Soc., Dalton Trans.*, 1987, Issue 1, pp. xvii—xx.

‡ However, there are exceptions: in $[Fe_3H(CO)_9(SC_3H_7)]$ the face-capping SC_3H_7 group restrains the metal triangle to be essentially equatorial.[4]

Table 1. Preliminary crystallographic data* for (**2**)—(**5**)

	(**2**)	(**3**)	(**4**)	(**4**)·xCH$_2$Cl$_2$	(**5**)
Source of crystals	Cooling EtOH solution	Diffusion of hexane into CH_2Cl_2 solution	Diffusion of Et_2O into MeCN solution	Diffusion of Et_2O into CH_2Cl_2 solution	Cooling MeOH solution
Lattice	Tetragonal I	Monoclinic P	Monoclinic P	Monoclinic P	Tetragonal P
a/Å	9.340(16)	8.205(3)	15.291(3)	13.591(2)	8.704(7)
b/Å	9.340(16)	16.011(4)	14.452(3)	28.390(5)	8.704(7)
c/Å	7.540(4)	13.975(2)	16.023(3)	18.208(3)	6.390(3)
β/°	90	101.87(4)	110.875(13)	93.412(14)	90
U/Å^3	658	1 797	3 308	7 013	485
Space group	N.d.	$P2_1/n$	Pn or $P2/n$	$P2_1/n$	N.d.
Z	2	4	4	8	2
D_c/g cm^{-3}	0.862	0.838	1.162	1.10 (x = 0), 1.26 (x = 1)	0.786
Reason for abandoning	No single space group allows the symmetry of the anion to be less than 4 or $\bar{4}$	Severe disorder in the propyl groups	Disorder of the anion even in the lower symmetry space group	Impossible satisfactorily to model disorder in the solvate molecules	Very poor crystal quality

* Mo-K_α radiation. N.d. = Not determined.

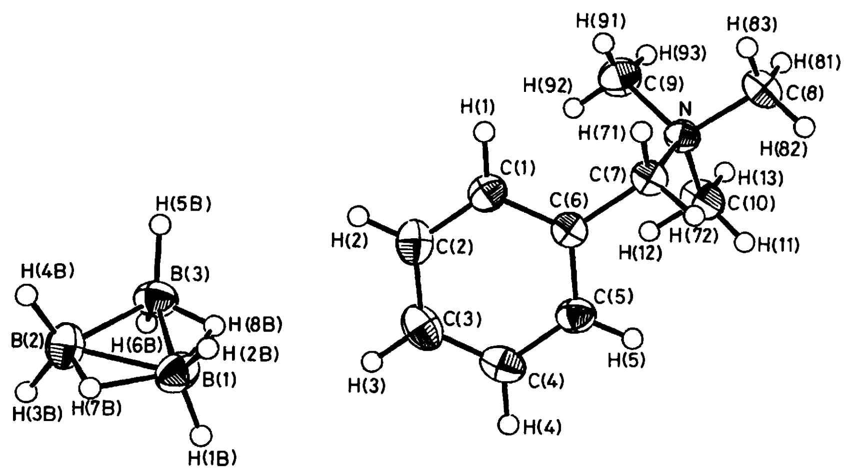

Figure 1. Molecular structure and numbering scheme in $[PhCH_2NMe_3][B_3H_8]$ (**1**). Thermal ellipsoids are drawn at the 50% probability level, except for H atoms which have an artificial radius of 0.1 Å for clarity

group $P2_1/c$, $Z = 4$, $D_c = 0.970$ g cm^{-3}, μ(Mo-K_α) = 0.49 cm^{-1}, $F(000) = 424$.

Data collection and processing. $\omega/2\theta$ scans in 96 steps with ω scan width (0.8 + 0.35 tan θ)°. Variable scan speeds dependent upon initial prescan. Graphite-monochromated Mo-K_α X-radiation, 4 183 reflections measured ($1 < \theta < 30°$, $+h+k+l$ and $-h+k+l$), 3 791 unique data, $R_{merge} = 0.0256$; 2 903 data with $F_o > 2.0\sigma(F_o)$ retained. No detectable crystal decay or movement throughout the data collection period.

Structure solution and refinement. Solved by direct methods (C and N atoms) and iterative full-matrix least-squares refinement and ΔF syntheses (B and H atoms). All non-H atoms allowed anisotropic thermal motion. Hydrogen atoms freely refined with individual isotropic thermal parameters. Weighting scheme, $w^{-1} = [\sigma^2(F_o) + 0.001\ 128\ F_o^2]$; $R = 0.0569$. $R' = 0.0773$, $S = 1.396$;* data:variables ratio 13:1. Maximum residue and minimum trough in final ΔF map 0.25 and -0.20 e Å^{-3}. Coefficients for analytical approximations to the atomic scattering factor curves were those inlaid in SHELX 76.[10] Computer programs used: CADABS,[11] SHELX 84,[12] SHELX 76, CALC,[13] and ORTEP-II.[14] Co-ordinates of refined atoms are listed in Table 2.

* $R = \Sigma|F_o - F_c|/\Sigma|F_o|$, $R' = [\Sigma w|F_o - F_c|^2/\Sigma w|F_o|^2]^{\frac{1}{2}}$, $S = [\Sigma w|F_o - F_c|^2/(\text{n.o.} - \text{n.v.})]^{\frac{1}{2}}$ (n.o. = no. of observations, n.v. = no. of variables).

Molecular Orbital Calculations.—For EMHO calculations, locally modified version of ICON8-FMO[15] using the weighted H_{ij} formula[16] and orbital exponents and H_{ii} values listed in Table 3. Orthogonalised Å co-ordinates of each of the models used are in SUP 56667. For MNDO calculations the package was used as supplied.[17] Orbital plotting *via* ORBIT[18] and a locally modified version of PSI 77.[19]

Results and Discussion

Crystal Structure of $[PhCH_2NMe_3][B_3H_8]$ (**1**).—A perspective view of an ion pair of (**1**) is shown in Figure 1 which also shows the atomic numbering scheme adopted. Bond lengths and angles in the $[B_3H_8]^-$ anion only are given in Table 4.

The species crystallises as well separated ion pairs with no significant inter-ion contacts. A unit-cell packing diagram is given in SUP 56667. The cation has effective C_s molecular symmetry and staggered conformations about all N–C bonds. Dimensions within the cation are unexceptional.

The $[B_3H_8]^-$ anion of (**1**) is characterised by the presence of two bridging hydrogen atoms, H(7B) and H(8B), lying within 0.1 Å of the plane of the B_3 triangle. The anion has approximate

Table 2. Fractional co-ordinates of refined atoms in $[PhCH_2NMe_3][B_3H_8]$ (**1**)

Atom	*x*	*y*	*z*	Atom	*x*	*y*	*z*
N	0.807 40(10)	0.166 91(11)	0.522 21(9)	H(71)	0.791 3(15)	0.318 4(19)	0.615 0(13)
C(1)	0.593 86(13)	0.200 43(14)	0.645 96(12)	H(72)	0.895 3(18)	0.212 8(19)	0.682 8(15)
C(2)	0.512 68(14)	0.134 78(17)	0.688 59(13)	H(81)	0.902 3(18)	0.217 6(21)	0.424 7(18)
C(3)	0.555 24(16)	0.022 60(16)	0.759 39(14)	H(82)	0.984 7(18)	0.228 8(19)	0.542 2(15)
C(4)	0.679 77(16)	−0.025 49(16)	0.787 65(13)	H(83)	0.878 3(16)	0.344 0(20)	0.486 4(14)
C(5)	0.761 58(14)	0.039 26(15)	0.744 45(11)	H(91)	0.660 1(18)	0.286 6(22)	0.445 4(15)
C(6)	0.719 76(12)	0.152 57(13)	0.673 48(10)	H(92)	0.620 4(16)	0.129 6(20)	0.453 9(14)
C(7)	0.809 75(13)	0.224 97(15)	0.630 02(11)	H(93)	0.684 4(20)	0.143(3)	0.366 2(18)
C(8)	0.903 85(16)	0.247 43(19)	0.491 13(14)	H(11)	0.930 8(19)	0.000 3(21)	0.594 6(18)
C(9)	0.678 64(16)	0.186 50(22)	0.435 85(13)	H(12)	0.777 6(18)	−0.036 4(22)	0.557 4(17)
C(10)	0.842 35(18)	0.014 40(16)	0.532 26(15)	H(13)	0.845 8(20)	−0.013 0(24)	0.466 6(20)
B(1)	0.299 78(16)	0.129 04(21)	0.897 78(15)	H(1B)	0.350 1(17)	0.038 9(20)	0.943 8(15)
B(2)	0.133 79(17)	0.141 23(20)	0.868 06(16)	H(2B)	0.355 5(21)	0.221(3)	0.911 2(19)
B(3)	0.192 44(19)	0.090 97(19)	0.763 21(14)	H(3B)	0.085 0(17)	0.052 4(21)	0.890 6(15)
H(1)	0.565 8(14)	0.278 1(17)	0.595 3(13)	H(4B)	0.081 0(19)	0.238 3(24)	0.847 1(18)
H(2)	0.425 1(19)	0.166 2(19)	0.667 7(15)	H(5B)	0.164 1(17)	0.168 6(20)	0.689 8(15)
H(3)	0.499 5(16)	−0.017 3(19)	0.792 8(14)	H(6B)	0.155 2(22)	−0.020(3)	0.737 2(21)
H(4)	0.707 9(16)	−0.111 3(20)	0.835 7(15)	H(7B)	0.214 6(22)	0.168 4(23)	0.945 9(19)
H(5)	0.847 0(17)	0.008 0(19)	0.761 4(15)	H(8B)	0.291(3)	0.082(3)	0.797 9(23)

Table 3. Parameters used in EHMO calculations

Orbital	H_{ii}/eV	ξ_1	ξ_2	c_1	c_2
H(1*s*)	−13.60	1.30			
B(2*s*)	−15.20	1.30			
B(2*p*)	−8.50	1.30			
C(2*s*)	−21.40	1.625			
C(2*p*)	−11.40	1.625			
O(2*s*)	−32.30	2.275			
O(2*p*)	−14.80	2.275			
Os(5*d*)	−12.42	5.650	2.417	0.6680	0.5885
Os(6*s*)	−10.36	2.450			
Os(6*p*)	−5.23	2.286			
Re(5*d*)	−12.66	5.343	2.277	0.6662	0.5910
Re(6*s*)	−9.36	2.398			
Re(6*p*)	−5.96	2.372			

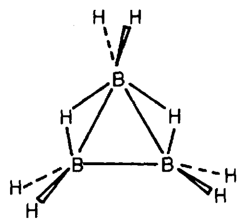

(**I**)

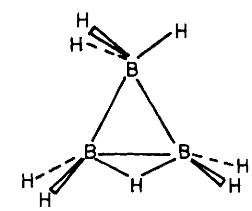

(**II**)

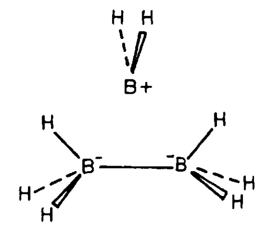

(**III**)

C_{2v} symmetry about the unique boron B(1). The important results of the structure determination in the context of our interest in the effects of H-bridging are that (*i*) the H-bridges are markedly asymmetric, and (*ii*) the bridged B–B bonds, B(1)–B(2) 1.760(3) and B(1)–B(3) 1.778(3) Å, are both substantially shorter than the unbridged one, B(2)–B(3) 1.804(3) Å.

The C_{2v} arrangement (**I**) of $[B_3H_8]^-$ has been shown by geometry-optimised *ab initio* m.o. calculations[7] to be only *ca.* 4 kJ mol^{-1} more stable than an alternative monobridged C_s form (**II**), and the equivalence of all eight hydrogen atoms in solution, at least on the n.m.r. time-scale, is well documented.[20] Such a small energy difference is well within the normal range of intermolecular forces in the solid state, and thus, whilst an earlier[6] crystallographic study of $[B_3H_8]^-$ as its $[H_2B(NH_3)_2]^+$ salt also indicated the dibridged C_{2v} structure, the monobridged form may yet be characterised by *X*-ray diffraction.

The structures of a number of derivatives of $[B_3H_8]^-$ have been determined in this laboratory and elsewhere. Examples exist of mono-[21,22] and di-bridged[23] forms and, in addition, some structures are found to be best described as intermediate, having one full and one partial hydrogen bridge.[24–26] Boron–boron bond lengths for these derivatives are given in Table 5. The pattern which clearly emerges from this compilation is one of H-bridging being associated with the shortest B–B connectivity, and this is fully consistent with the optimised structures for $[B_3H_8]^-$ in mono- and di-bridged forms of McKee and Lipscomb.[7]

In (**1**) H(7B) and H(8B) each bridge their respective B–B connectivities asymmetrically, being 1.38 and 1.36 Å from B(1), and 1.12 and 1.03 Å from B(2) and B(3), *cf.* 1.05—1.17 Å for the six terminal B–H bond lengths. To accommodate the relatively short B(2,3)–H(7B,8B) bonds the H atoms terminal to B(2) and B(3) are bent towards each other, resulting in narrower H(3—6)–B(2,3)–B(3,2) angles than H(1,2)–B(1)–B(2,3) angles. This affords the extreme view of the $[B_3H_8]^-$ anion as (**III**), an adduct between eclipsed $[B_2H_6]^{2-}$ and angular $[BH_2]^+$, the latter approaching along one of the C_2 axes of the former to make only two short B–H contacts. Although this simple description is in accord with the relative charges calculated[27] for the two kinds of boron atom it does not easily lead to an understanding of the relative lengths of bridged *versus* unbridged B–B bonds.

Therefore we have adopted an alternative method of fragmenting the $[B_3H_8]^-$ ion to understand the effects of H-bridging, and have used the same approach for other bridged borane and transition-metal clusters, as described in the following section.

Molecular Orbital Calculations.—To rationalise the consequences of H-bridging on B–B and M–M lengths one must

Table 4. Bond lengths (Å) and angles (°) in the $[B_3H_8]^-$ anion of (**1**)

B(1)–B(2)	1.760(3)	B(1)–H(7B)	1.382(24)	B(2)–H(3B)	1.104(20)	B(3)–H(5B)	1.165(20)
B(1)–B(3)	1.778(3)	B(1)–H(8B)	1.36(3)	B(2)–H(4B)	1.075(23)	B(3)–H(6B)	1.14(3)
B(1)–H(1B)	1.080(19)	B(2)–B(3)	1.804(3)	B(2)–H(7B)	1.121(24)	B(3)–H(8B)	1.03(3)
B(1)–H(2B)	1.048(24)						

B(2)–B(1)–B(3)	61.32(11)	H(1B)–B(1)–H(7B)	105.2(14)	B(3)–B(2)–H(3B)	111.3(10)	B(1)–B(3)–H(8B)	49.9(16)
B(2)–B(1)–H(1B)	117.9(10)	H(1B)–B(1)–H(8B)	96.9(16)	B(3)–B(2)–H(4B)	110.6(12)	B(2)–B(3)–H(5B)	114.1(10)
B(2)–B(1)–H(2B)	119.9(13)	H(2B)–B(1)–H(7B)	99.7(17)	B(3)–B(2)–H(7B)	111.4(13)	B(2)–B(3)–H(6B)	106.2(13)
B(2)–B(1)–H(7B)	39.6(10)	H(2B)–B(1)–H(8B)	105.2(18)	H(3B)–B(2)–H(4B)	116.2(16)	B(2)–B(3)–H(8B)	108.5(16)
B(2)–B(1)–H(8B)	96.6(12)	H(7B)–B(1)–H(8B)	136.2(16)	H(3B)–B(2)–H(7B)	103.9(16)	H(5B)–B(3)–H(6B)	112.2(16)
B(3)–B(1)–H(1B)	115.0(10)	B(1)–B(2)–B(3)	59.82(11)	H(4B)–B(2)–H(7B)	102.8(17)	H(5B)–B(3)–H(8B)	109.9(19)
B(3)–B(1)–H(2B)	118.7(13)	B(1)–B(2)–H(3B)	118.6(10)	B(1)–B(3)–B(2)	58.85(11)	H(6B)–B(3)–H(8B)	105.5(21)
B(3)–B(1)–H(7B)	100.8(10)	B(1)–B(2)–H(4B)	123.5(12)	B(1)–B(3)–H(5B)	125.5(10)	B(1)–H(7B)–B(2)	88.7(16)
B(3)–B(1)–H(8B)	35.4(12)	B(1)–B(2)–H(7B)	51.7(12)	B(1)–B(3)–H(6B)	121.8(13)	B(1)–H(8B)–B(3)	94.7(21)
H(1B)–B(1)–H(2B)	114.0(17)						

Table 5. Boron–boron distances (Å) in $[B_3H_8]^-$ and its derivatives $[B_3H_7X]^-$

X	Bridged B–B	Intermediate B–B	Unbridged B–B	Ref.
CO^a	1.75(1)		1.83(1), 1.86(1)	21
$NCBH_3$	1.718(7)		1.833(7), 1.840(7)	22
NCB_3H_7 or CNB_3H_7	1.710(10)		1.804(10), 1.813(9)	22
	1.715(10)		1.815(10), 1.833(11)	
$NCAgCNB_3H_7{}^b$	1.75(3)		1.801(21), 1.829(24)	22
	1.687(24)	1.815(23)	1.809(12)	
NH_3	1.744(5)	1.803(6)	1.820(6)	24
NCS	1.760(5)	1.793(6)	1.807(5)	25
NCSe	1.763(8)	1.788(8)	1.794(8)	25
$CH_2PPh_3{}^+$	1.766(9)	1.793(9)	1.816(9)	26
H	1.77		1.80	6
H	1.760(3), 1.778(3)		1.804(3)	*c*
$Cl_2{}^d$	1.754(16), 1.763(16)		1.804(13)	23

[a] Mean of two independent molecules. [b] One $\{B_3H_7\}$ fragment is monobridged, the other intermediate. [c] This work. [d] Disubstituted derivative [*trans*-1,2-Cl_2-$B_3H_6]^-$; bridged bonds are B(1)–B(3) and B(2)–B(3).

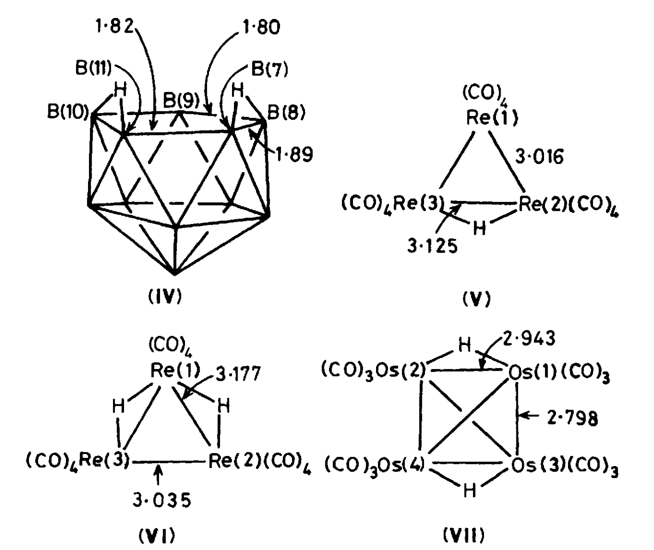

Figure 2. Some examples of clusters in which H-bridging is associated with a lengthening of the bridged bond (distances in Å)

consider molecules in which the presence or absence of H-bridges represents the only difference between otherwise equivalent connectivities. Thus, although the bridged connectivity of (**II**) is shorter than the unbridged connectivities, this species is not a strictly valid example of a structure in which H-bridging can be said to be associated with a difference in edge length. $[B_3H_8]^-$ in the C_{2v} form (**I**) is a suitable candidate, whose *X*-ray structure, confirmed above, shows that H-bridging is associated with *shortening* of the bridged B–B bonds.

In contrast, $[B_{11}H_{13}]^{2-}$ (**IV**) displays[28] *lengthening* of the bridged connectivities relative to otherwise equivalent ones (Figure 2). Many transition-metal cluster compounds also have edge-bridging H atoms whose effect seems to be a lengthening of the bridged bond, and Figure 2 shows line diagrams and important bond lengths (averaged over equivalent connectivities where appropriate) for some typical examples. Hydrogen atoms were not located in crystallographic studies of $[Re_3H(CO)_{12}]^{2-}$ (**V**),[29] $[Re_3H_2(CO)_{12}]^-$ (**VI**),[30] and $[Os_4H_2(CO)_{12}]^{2-}$ (**VII**),[31] but analysis of the disposition of the carbonyl ligands allowed confident prediction of the H-atom location(s) in each case. These molecules are suitable for this study since, again, bridged and unbridged bonds are otherwise chemically equivalent.

In all cases we have approached the problem by considering the perturbation of a high-symmetry anion as a consequence of protonation. For example, in the case of (**I**) we have doubly edge-protonated the D_{3h} species $[B_3H_6]^{3-}$ and traced the origins of its subsequent deformation. This approach is particularly rewarding in a comparison of (**I**) with (**VI**), since the anions $[B_3H_6]^{3-}$ and $[Re_3(CO)_{12}]^{3-}$ are composed of isolobal–isoelectronic C_{2v} $\{BH_2\}^-$ and C_{4v} $\{Re(CO)_4\}^-$ fragments, yet double protonation of the former trianion results in B–B bond shortening whilst similar protonation of the latter trianion results in Re–Re bond lengthening.

Finally, we have re-examined the B–B edge protonation of

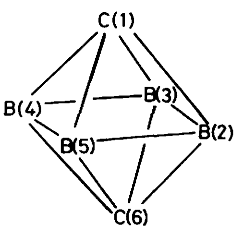

(VIII)

closo-1,6-$C_2B_4H_6$ (**VIII**) at the (geometry-optimised) MNDO level of calculation. This system is less attractive than those discussed above in that no experimental proof of the effect of protonation is available to check the validity of the theoretical arguments. It nevertheless aroused our interest since DeKock and Jasperse[8] report that symmetric H-bridging is predicted to result, unusually, in a contraction of the bridged B–B edge.

$$[B_{11}H_{11}]^{4-}(C_{5v}) + 2H^+ \longrightarrow [B_{11}H_{13}]^{2-}(C_s) \quad (1)$$

The orbitals of the $\{B_{11}H_{11}\}$ fragment have been described previously.[32] A partial interaction diagram for equation (1) is shown in Figure 3. For the sake of clarity constructions are only drawn if the coefficient of the fragment molecular orbital (f.m.o.) in the m.o. is >0.3. Interfragment overlap integrals >0.2 are $<5E_1/\Sigma_u^+> 0.4958$, $<5A_1/\Sigma_g^+> 0.2741$, $<2E_1/\Sigma_u^+> 0.2634$, $<2A_1/\Sigma_g^+> 0.3596$, $<1E_1/\Sigma_u^+> 0.2951$, and $<1A_1/\Sigma_g^+> 0.3099$.

On passing from C_{5v} $[B_{11}H_{11}]^{4-}$ to C_s $[B_{11}H_{13}]^{2-}$ the f.m.o.s of the cage which are of A_1 symmetry interact with the Σ_g^+ combination of the $[H\cdots H]^{2+}$ fragment. The degeneracies of the E_1 pairs of $[B_{11}H_{11}]^{4-}$ are lifted with that component having a nodal plane close to the protons being effectively unaltered in the dianion. The other component interacts with Σ_u^+ to afford A'' m.o.s. The E_2 orbitals of $[B_{11}H_{11}]^{4-}$ effectively have zero net overlap with the $[H\cdots H]^{2+}$ group orbitals since the protons are close to one of their nodal planes. Figure 3 clearly shows a three-orbital interaction with components of $5E_1$ and $3E_1$ mixing with Σ_u^+ to give the occupied m.o.s $6A''$ and $5A''$ in $[B_{11}H_{13}]^{2-}$. The strongly antibonding combination $10A''$ is high lying and unoccupied. The $5E_1$ and, to a lesser extent, the $3E_1$ orbital of $[B_{11}H_{11}]^{4-}$ are localised on, and are outpointing from, the pentagonal polyhedral face.[32]

Examination of the cage f.m.o. occupations in the dianion reveals the essential reason for the relative lengthening of the bridged connectivities B(7)–B(8) and B(10)–B(11). Occupations of all the previously filled orbitals are >1.8 e except for $6A_1$ (1.45 e) and one component of $5E_1$ (1.15 e). Deoccupation of the former would not be expected to reduce the symmetry of the $\{B_{11}\}$ fragment in the dianion. In contrast, asymmetric occupation of a formally equally occupied E_1 pair must lead to a molecular Jahn-Teller distortion. The orbitals $5E_1$, the highest occupied molecular orbitals (h.o.m.o.s) of $[B_{11}H_{11}]^{4-}$, are drawn in Figure 4. The component, (*b*), which becomes preferentially deoccupied in $[B_{11}H_{13}]^{2-}$ is π-bonding along B(7)–B(8) and B(10)–B(11), and π-antibonding between B(7)–B(11) and B(8)$\cdots$B(10). The effect of its deoccupation will clearly be to lengthen the former pair of connectivities relative to the latter pair, and this is in full accord with the structure of (**IV**) determined crystallographically.[28]

$$[Os_4(CO)_{12}]^{4-}(T_d) + 2H^+ \longrightarrow [Os_4H_2(CO)_{12}]^{2-}(D_{2d}) \quad (2)$$

Interaction diagrams for the protonations (2)—(4) are very crowded due to intense concentrations of f.m.o.s and m.o.s

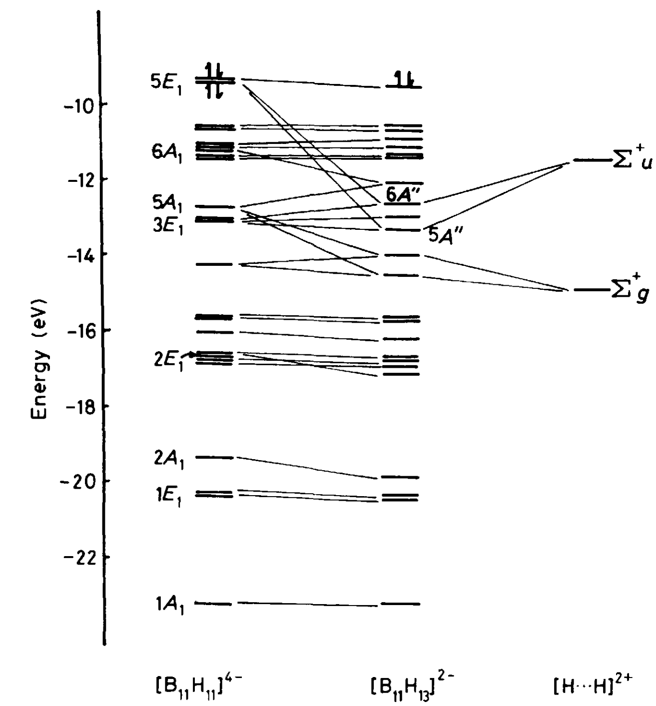

Figure 3. Interaction diagram for the double protonation of $[B_{11}H_{11}]^{4-}$. Only filled orbitals of this and the product $[B_{11}H_{13}]^{2-}$ are shown (eV $\approx 1.60 \times 10^{-19}$ J)

arising from the *d* orbitals of the transition-metal atoms, and are therefore largely uninformative for the present purposes. However, an understanding of the observed lengthening of the bridged Os–Os bonds relative to unbridged ones in (**VII**) is afforded, again, by following the occupations of the f.m.o.s of the tetra-anion as it is protonated.

Upon simultaneous Os(1)–Os(2) and Os(3)–Os(4) edge protonation the f.m.o.s of $[Os_4(CO)_{12}]^{4-}$ that are deoccupied by >0.2 e are one component each of $6E$ (occupation 1.79 e), $12T_2$ (1.02 e), and $7E$ (second h.o.m.o., 1.27 e). All these fragment orbitals have >70% metal character.

Views of the tetra-anion f.m.o.s for which deoccupation is the most marked are presented in Figure 5; (*a*) is the active component of $7E$ and (*c*), that of $12T_2$. Both are strongly σ-bonding along the Os(1)–Os(2) and Os(3)–Os(4) edges, and consequently their deoccupation would be expected to result in the bridged-bond lengthening that is observed.[31] In contrast, point-group symmetry demands that the other component of $7E$, Figure 5(*b*), and other components of $12T_2$, be noded at $\mu_{1,2}$-H and $\mu_{3,4}$-H positions, and must therefore remain fully occupied in the protonated complex.

$$[Re_3(CO)_{12}]^{3-}(D_{3h}) + H^+ \longrightarrow [Re_3H(CO)_{12}]^{2-}(C_{2v}) \quad (3)$$

A single μ-H atom can only interact by symmetry with those f.m.o.s of $[Re_3(CO)_{12}]^{3-}$ that are of A_1 symmetry and those components of E' pairs that are not noded through the H-atom position.

EHMO calculations show that the only filled f.m.o. of the trianion whose occupation changes by >0.2 e on protonation of the Re(2)–Re(3) edge is the appropriate component, Figure 6(*a*), of $15E'$, the occupation decreasing to 1.30 e. The $15E'$ orbitals, which lie only slightly below $10A_1$ {the h.o.m.o. of $[Re_3(CO)_{12}]^{3-}$}, are plotted in Figure 6, with (*a*) relevant to (**V**). The component in Figure 6(*a*) is strongly σ-bonding between Re(2)

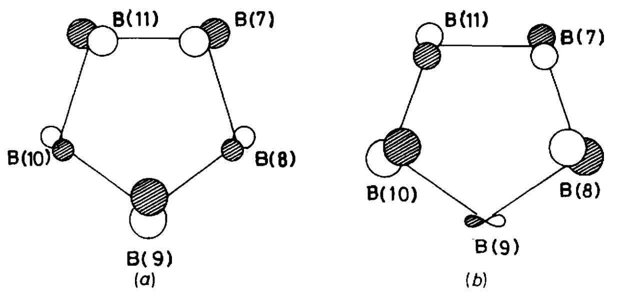

Figure 4. Components of the $5E_1$ set of $[B_{11}H_{11}]^{4-}$, viewed from a point directly above the open polyhedral face. Only B atoms in the open face, and no H atoms, are shown

Table 6. Variation of the $\langle 2E'(a)/\Sigma_g^+\rangle$ and $\langle 2E'(b)/\Sigma_u^+\rangle$ overlap integrals with shift (σ) of the μ-H atoms in $[B_3H_8]^-$

σ/Å	0.00	0.20	0.40	0.60
$\langle 2E'(a)/\Sigma_g^+\rangle$	0.3923	0.4511	0.4903	0.5056
$\langle 2E'(b)/\Sigma_u^+\rangle$	0.7127	0.6558	0.5764	0.4770

and Re(3), and therefore single protonation of $[Re_3(CO)_{12}]^{3-}$ results in the lengthening of the bridged bond that is observed crystallographically.[29]

$$[Re_3(CO)_{12}]^{3-} (D_{3h}) + 2H^+ \longrightarrow [Re_3H_2(CO)_{12}]^- (C_{2v}) \quad (4)$$

The only orbitals of $[Re_3(CO)_{12}]^{3-}$ that undergo a substantial change in occupation upon double protonation [Re(1)–Re(2) and Re(1)–Re(3) edges] are $10A_1$ (h.o.m.o., 2.00 e $\longrightarrow$ 1.60 e) and $15E'$ (second h.o.m.o., 2 × 2.00 e $\longrightarrow$ 1.63 e and 1.01 e). Again, reduction in fragment symmetry will only result from the latter uneven occupation. This time the component of $15E'$ which becomes the less occupied is Figure 6(*b*). This orbital is σ-bonding in character along the Re(1)–Re(2) and Re(1)–Re(3) bonds, and is π-antibonding between Re(2) and Re(3). Consequently, the effect of protonation of the Re(1)–Re(2) and Re(1)–Re(3) edges will be to cause their lengthening relative to the unbridged Re(2)–Re(3), as determined by the crystallographic study[31] of (**VI**).

$$[B_3H_6]^{3-} (D_{3h}) + 2H^+ \longrightarrow [B_3H_8]^- (C_{2v}) \quad (5)$$

A partial interaction diagram for this system, in which the μ-H atoms *symmetrically* bridge the B(1)–B(2) and B(1)–B(3) connectivities, is given in Figure 7. Again f.m.o.s and m.o.s are linked only if the coefficient of the former in the latter is >0.3. The interfragment overlap integrals are $<2E'/\Sigma_g^+> 0.3923$, $<2E'/\Sigma_u^+> 0.7127$, $<2A_1'/\Sigma_g^+> 0.1704$, $<1E'/\Sigma_g^+> 0.1903$, $<1E'/\Sigma_u^+> 0.3458$, and $<1A'/\Sigma_g^+> 0.5559$.

On passing from D_{3h} $[B_3H_6]^{3-}$ to C_{2v} $[B_3H_8]^-$ [equation (5)] there is substantial mixing of the $2E'$ and $2A'$ f.m.o.s to afford $6A'$, $5A'$, and $3A''$ m.o.s, the last two also involving large components of the symmetric and antisymmetric $[H\cdots H]^{2+}$ group orbitals respectively. The $2E'$ f.m.o.s are sketched in Figure 8. Note their resemblance to $15E'$ of $[Re_3(CO)_{12}]^{3-}$ (Figure 6).

Inspection of the occupancies of the f.m.o.s of $[B_3H_6]^{3-}$ in $[B_3H_8]^-$ reveals that *symmetric* H-bridging causes both components of $2E'$ to be substantially deoccupied, component (*a*) falling to 1.30 e, and (*b*) to 0.94 e. Clearly, the consequence of this asymmetric occupation would be to cause the bridged connectivities to *lengthen* relative to the unbridged one, as in the related species $[Re_3H_2(CO)_{12}]^-$. This is in disagreement with the observed asymmetry in the B–B lengths determined in the above crystallographic study.

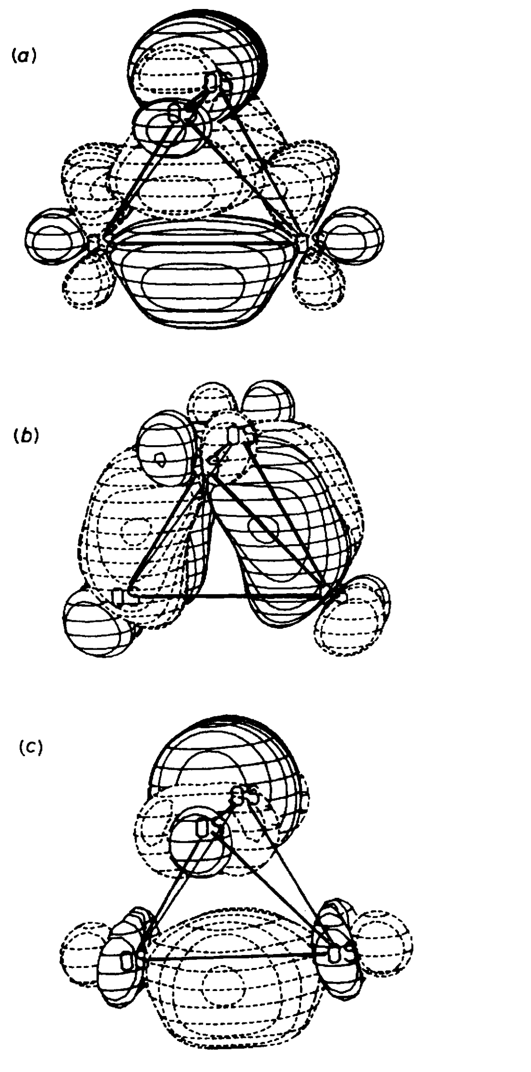

Figure 5. Three-dimensional plots of selected orbitals of $[Os_4(CO)_{12}]^{4-}$: Os(1) and Os(2) are on the upper edge of the tetrahedron, and Os(3) and Os(4) are on the lower edge; (*a*), (*b*) components of $7E$; (*c*) one component of $12T_2$

However, a fundamental difference between the *X*-ray-determined structure and the theoretical model used above is that in the former the μ-H atoms clearly *do not* symmetrically bridge the B–B edges. From the form of the $2E'$ orbitals in Figure 8 it is apparent that movement of the μ-H atoms parallel to the bridged edges, towards B(2) and B(3), will result in increasing interaction between Σ_g^+ and $2E'(a)$ at the expense of the $\Sigma_u^+/2E'(b)$ interaction. This is confirmed by the relevant overlap integrals in Table 6, where σ is the shift of the μ-H atoms from their symmetric positions.

Increasing interaction of the (filled) $2E'(a)$ orbital of $[B_3H_6]^{3-}$ with the (empty) Σ_g^+ group orbital of $[H\cdots H]^{2+}$ leads to the decreasing occupation of the former in the molecule, and a switch in the relative occupations of components (*a*) and (*b*) would lead naturally to bridged bond *shortening* compared to the unbridged bond. Figure 9 plots the f.m.o. occupation of $2E'$ of $[B_3H_6]^{3-}$ in $[B_3H_8]^-$ *versus* σ. The switch occurs at σ *ca.* 0.6 Å, which corresponds to B(1)–μ-H = 1.74 and B(2),B(3)–μ-H = 0.94 Å. Although the discrepancy in B–μ-H lengths here is obviously greater than that actually observed, the

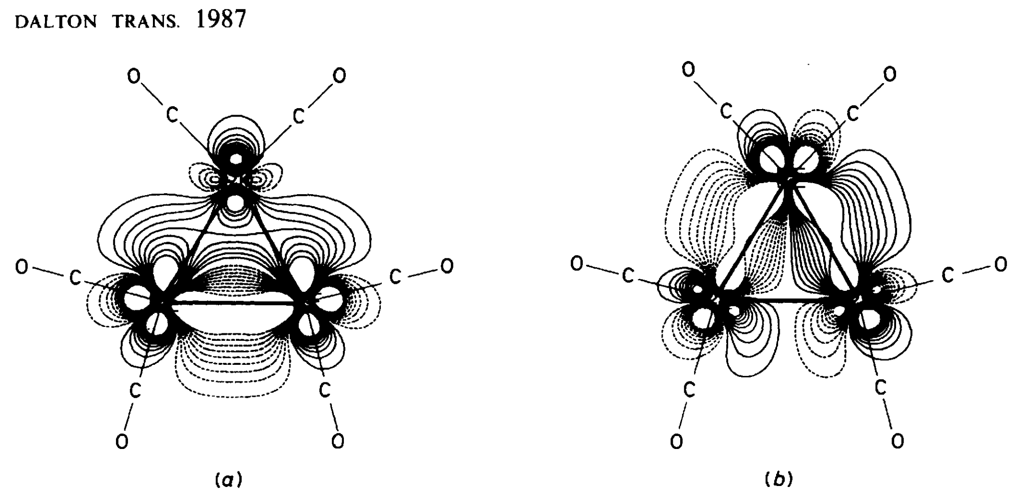

Figure 6. Two-dimensional (Re_3 plane) plots of the $15E'$ orbitals of $[Re_3(CO)_{12}]^{3-}$: Re(1) is the upper apex of the triangle and Re(2) and Re(3) are the basal atoms

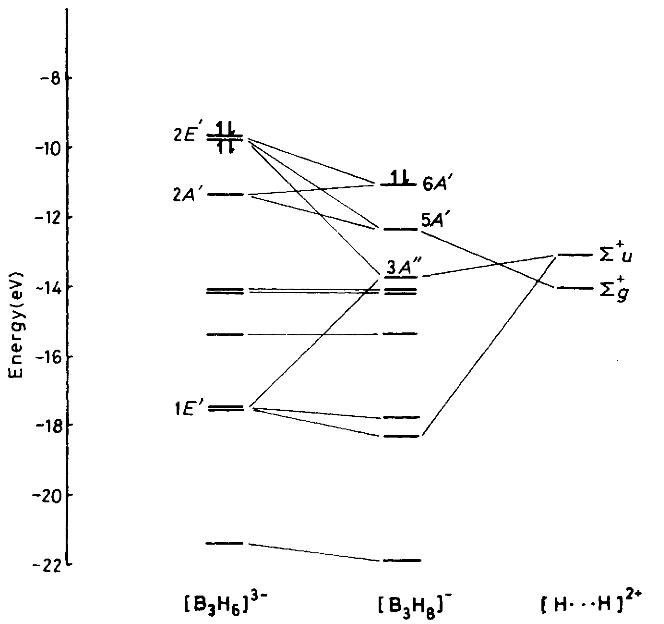

Figure 7. Interaction diagram for symmetric H-bridging in $[B_3H_8]^-$. Only filled $[B_3H_6]^{3-}$ and $[B_3H_8]^-$ orbitals are shown

correlation that is suggested between the asymmetry in the H-bridges and the asymmetry in the B–B lengths is in *qualitative* agreement with that noted in the experimentally determined structure. Given the inadequacies of the EHMO method and the assumptions in the models employed in the calculations, imprecise agreement is not serious. One important point is that we have used an equilateral B_3 triangle. Once the triangle begins to distort to C_{2v}-isosceles [B(1)–B(2), B(1)–B(3) < B(2)–B(3)] the B_1 f.m.o. derived from $2E'(a)$ lies at higher energy than the B_2 orbital derived from $2E'(b)$ and would therefore have reduced overlap with Σ_g^+, reducing the driving force towards further asymmetry in the H-bridges. Thus, not only are the two notable asymmetries in $[B_3H_8]^-$ (B–B connectivities and the position of the μ-H atoms) highly correlated, but they are also mutually self-regulating.

Finally, we note that shifting the μ-H atoms to $\sigma = 0.6$ Å in $[B_3H_8]^-$ also results in a difference in occupation between the components of $1E'$ of $[B_3H_6]^{3-}$. These are essentially B–H$_{\text{terminal}}$

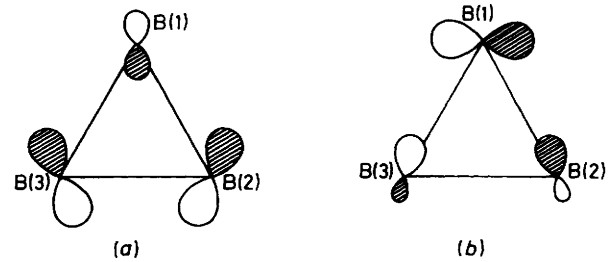

Figure 8. The $2E'$ orbitals of $[B_3H_6]^{3-}$, with H atoms omitted

bonding orbitals, and are sketched in Figure 10. Component (*b*), antibonding between the {B(2)H$_2$} and {B(3)H$_2$} fragments, becomes partially deoccupied (1.73 e) at $\sigma = 0.6$ Å [*cf.* component (*a*), 1.99 e]. This specific deoccupation of $1E'(b)$ will tend to oppose the relative shortening of the B(1)–B(2) and B(1)–B(3) bonds upon μ-H shift, but its effect in this sense will be relatively small. It does, however, nicely account for the bending towards each other of the H atoms terminal to B(2) and B(3) that is observed in the crystallographic study.

$$1,6\text{-}C_2B_4H_6\ (D_{4h}) + H^+ \longrightarrow [C_2B_4H_7]^+\ (C_{2v}) \quad (6)$$

DeKock and Jasperse[8] have carried out a theoretical study of this edge protonation. They report, using geometry-optimised MNDO calculations, that $\mu_{2,3}$ protonation of 1,6-$C_2B_4H_6$ [equation (6)] results in a structure in which the bridged B–B connectivity (1.66 Å) is shorter than the adjacent [B(3)–B(4) and B(2)–B(5), 1.84 Å] and opposite [B(4)–B(5), 1.91 Å] edges, and they discuss this unusual result in terms of the specific interaction between H^+ and the h.o.m.o. of 1,6-$C_2B_4H_6$ (B_{1g}, bonding with respect to all B–B edges).

EHMO–FMO calculations on $[C_2B_4H_7]^+$ show that the only f.m.o.s of $C_2B_4H_6$ whose occupancy changes by >0.05 e on B(2)–B(3) edge protonation are $1B_{1g}$ (the h.o.m.o., occupancy 1.01 e) and component (*a*) of $1E_u$ (occupancy 1.87 e).

The $1E_u(a)$ orbital is sketched in Figure 11(*a*). It is composed of B(2*s*) and H(1*s*) character, being net B–B non-bonding but bonding with respect to all B–H$_{\text{terminal}}$ interactions. Importantly it is bonding between B(2) and B(3). However, it's deoccupation in the protonated complex is small compared to typical deoccupations noted above, and we would therefore expect a *slight lengthening* of B(2)–B(3) [and B(4)–B(5)] upon edge protonation. Since this is the opposite prediction to that of

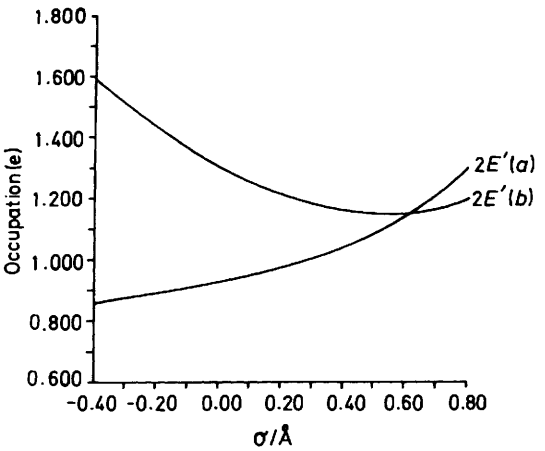

Figure 9. Changes in the occupation of the $2E'$ orbitals of $[B_3H_6]^{3-}$ in $[B_3H_8]^-$ as a function of σ, the shift of the μ-H atoms of the latter

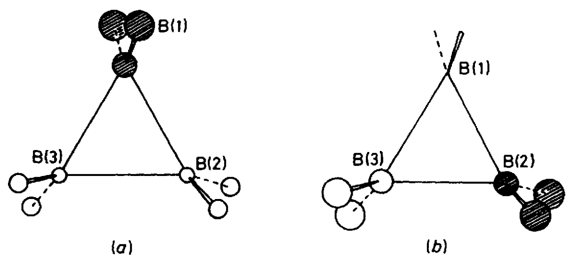

Figure 10. The $1E'$ orbitals of $[B_3H_6]^{3-}$

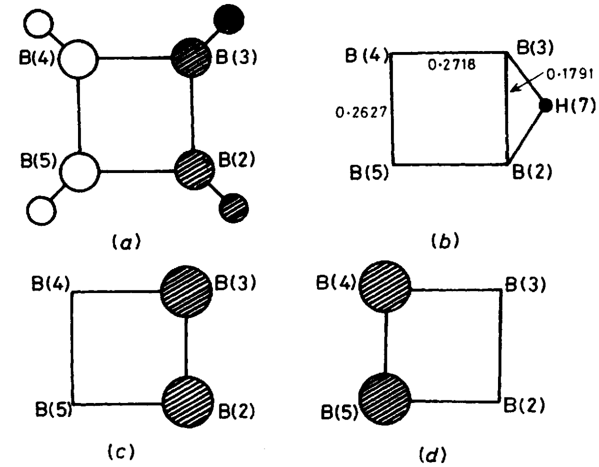

Figure 11. (*a*) Component $1E_u(a)$ orbital of $C_2B_4H_6$; (*b*) reduced overlap populations in $[C_2B_4H_7]^+$ [the μ-H atom bridges the B(2)–B(3) bond]; (*c*), (*d*) linear combinations of $1E_u(a)$ and $2A_{1g}$ of $C_2B_4H_6$

DeKock and Jasperse[8] we have reinvestigated both $C_2B_4H_6$ and $[C_2B_4H_7]^+$ *via* MNDO calculations. Note that in our calculations C_{2v} symmetry only was imposed on both species.

Optimised orthogonalised Å co-ordinates for both species are in SUP 56667. We agree with DeKock and Jasperse that the apparent equilibrium geometry of the protonated form is asymmetric, with B(2)–B(3) < B(3)–B(4), B(2)–B(5) < B(4)–B(5), and we reproduce their bond lengths almost exactly. However, the geometry-optimised calculation on $C_2B_4H_6$ (omitted from the work of DeKock and Jasperse[8]) affords an equilibrium geometry which is similarly asymmetric, but more so. Specifically, in this species B(2)–B(3) = 1.52, B(3)–B(4), B(2)–B(5) = 1.84, and B(4)–B(5) = 1.90 Å.

The compound 1,6-$C_2B_4H_6$ is known[33] to have a D_{4h} (pseudo-octahedral) geometry. Clearly the MNDO-optimised structure in which only C_{2v} symmetry is imposed is incorrect; the reasons for this are well documented.[34–36] Unfortunately DeKock and Jasperse have compared the C_{2v}-optimised structure of $[C_2B_4H_7]^+$ with a D_{4h}-optimised structure of $C_2B_4H_6$. Given the inadequacies of the MNDO method for molecules with multicentre bonding a comparison between optimised structures so derived is clearly inappropriate since the structural 'changes' in $[C_2B_4H_7]^+$ are largely attributable to the decreased symmetry constraints. However, it is still valid to compare the structures of neutral and protonated analogues optimised by MNDO *in the same point group*. In this case the only real structural change is a *lengthening* (0.14 Å) of the protonated B–B edge.

Reduced overlap populations in $[C_2B_4H_7]^+$ calculated by the EHMO method are shown in Figure 11(*b*). They are clearly consistent with B(2)–B(3) being the longest B–B connectivity in the protonated form. In C_{2v} $[C_2B_4H_7]^+$, B(2)–B(3) is no longer symmetry-equivalent to B(4)–B(5), but this is not reflected in the simple depopulation analysis reported above, which suggests only a rectangular and not a trapezoidal distortion of the B_4 square.

The overlap populations of $[C_2B_4H_7]^+$ are best understood by constructing localised orbitals from the m.o.s of $C_2B_4H_6$. On passing from D_{4h} $C_2B_4H_6$ to C_{2v} $[C_2B_4H_7]^+$, $1E_u(a)$ and $2A_{1g}$ of the former mix to produce in-phase and out-of-phase (A_1) combinations, Figure 11(*c*) and (*d*) respectively, of which only the former is substantially deoccupied upon B(2)–B(3) edge protonation.

Conclusions

Structures are known for a number of clusters in which H-bridging is the only difference between otherwise chemically equivalent connectivities. In all of these except $[B_3H_8]^-$, H-bridging is symmetric and is associated with relative lengthening of the bridged bond. We have shown that this results from an unequal occupation of degenerate orbitals* of the deprotonated form upon protonation.

In $[B_3H_8]^-$ the H-bridges are markedly asymmetric. Asymmetric double protonation causes a reversal in the deoccupations of the $2E'$ orbitals of $[B_3H_6]^{3-}$ relative to that if the bridges were symmetric. The reversal results in bridged bond shortening.

The vast majority of clusters containing H-bridges unfortunately do not contain connectivities whose only difference is the presence or absence of the bridge, and so lack a suitable built-in reference. In such cases it is clear that one cannot be certain that any observed differences in the lengths of bridged and unbridged bonds are largely due to the H-bridge. Consequently the value of the assignment of μ-H atom positions on

* In some cases, *e.g.* $[Re_3(CO)_{12}]^{3-}$, the active components of the degenerate sets of f.m.o.s are already sufficiently localised for the effects of protonation to be obvious. In others the canonical m.o.s *are not* adequately localised on the bonds to be contrasted, and in these cases it is necessary to construct linear combinations of the former. Thus for deprotonated molecules such as $[Os_3H(CH_2)(CO)_{10}]^-$,[37] in which the point group is non-degenerate, this procedure is required to produce the necessary degeneracy and localisation. In cases like $C_2B_4H_6$ partial distinction between bridged and unbridged bonds can be made immediately, but the construction of linear combinations is then needed to contrast, *e.g.* the B(2)–B(3) and B(4)–B(5) connectivities.

the basis of relative lengths alone is doubtful in clusters of this type. It is nevertheless still reasonable to attempt to answer the question of the influence of H-bridging on the length of a B–B or M–M bond in such molecules. A precise answer depends, however, on a rather more precise question, since there are in principle three ways of 'adding' a symmetric μ-H function to such a bond. (*i*) Addition of H^+ must cause a localised two-centre, two-electron B–B or M–M bonding f.m.o. to become partially deoccupied in forming a bonding three-centre, two-electron interaction, and would therefore result in bond lengthening. (*ii*) Addition of H converts a two-centre, one-electron bond into a three-centre, two-electron bond. Its effect on bond length is expected to be small. (*iii*) Addition of H^- will partially occupy an orbital of the cluster that was previously B–B or M–M bonding but empty. This must cause bond shortening.

In chemical reactions μ-H atoms are invariably added to, or abstracted from, clusters as protons. Therefore the only comparison that is feasible (in cases where otherwise chemically equivalent bridged and unbridged connectivities do not exist) is that between B–B or M–M bond lengths in protonated and deprotonated analogues, assuming no gross structural changes.[38] In such cases the available evidence is that symmetric μ-H^+ addition causes the bridged bond to lengthen.

Acknowledgements

We thank the S.E.R.C. for a postgraduate studentship (to G. F. M.) and Dr. J. H. Morris for crystals of the CH_2Cl_2 solvate of $[N(PPh_3)_2][B_3H_8]$.

References

1 M. R. Churchill, B. G. DeBoer, and F. J. Rotella, *Inorg. Chem.*, 1976, **15**, 1843.
2 P. R. Raithby, in 'Transition Metal Clusters,' ed. B. F. G. Johnson, Wiley, Chichester, 1980, pp. 5—192.
3 L. Barton, *Top. Curr. Chem.*, 1982, **100**, 169.
4 R. Bau, B. Don, R. Greatrex, R. J. Haines, R. A. Love, and R. D. Wilson, *Inorg. Chem.*, 1975, **14**, 3021.
5 See, for example, P. D. Boyle, B. J. Johnson, A. Buehler, and L. H. Pignolet, *Inorg. Chem.*, 1986, **25**, 7.
6 C. R. Peters and C. E. Nordman, *J. Am. Chem. Soc.*, 1960, **82**, 5758.
7 M. L. McKee and W. N. Lipscomb, *Inorg. Chem.*, 1982, **21**, 2846.
8 R. L. DeKock and C. P. Jasperse, *Inorg. Chem.*, 1983, **22**, 3843.
9 E. Amberger and E. Gut, *Chem. Ber.*, 1968, **101**, 1200.
10 G. M. Sheldrick, SHELX 76, University of Cambridge, 1976.
11 R. O. Gould, CADABS, University of Edinburgh, 1985.
12 G. M. Sheldrick, SHELX 84, University of Göttingen, Federal Republic of Germany, 1984.
13 R. O. Gould and P. Taylor, CALC, University of Edinburgh, 1986.
14 C. K. Johnson, ORTEP-II, Report ORNL-5138, Oak Ridge National Laboratory, Tennessee, U.S.A., 1976.
15 J. Howell, A. Rossi, D. Wallace, K. Haraki, and R. Hoffmann, ICON, Quantum Chemistry Program Exchange, University of Indiana, 1977, no. 344.
16 J. H. Ammeter, H-B. Burgi, J. C. Thibeault, and R. Hoffmann, *J. Am. Chem. Soc.*, 1982, **100**, 3686.
17 W. Thiel, MNDO, Quantum Chemistry Program Exchange, University of Indiana, 1977, no. 353.
18 G. F. Mitchell, ORBIT, University of Edinburgh, 1983.
19 W. L. Jorgensen, PSI 77, Quantum Chemistry Program Exchange, University of Indiana, 1977, no. 340.
20 W. C. Phillips, H. C. Miller, and E. L. Muetterties, *J. Am. Chem. Soc.*, 1959, **81**, 4496.
21 J. D. Glore, J. W. Rathke, and R. Schaeffer, *Inorg. Chem.*, 1973, **12**, 2175.
22 S. J. Andrews and A. J. Welch, *Inorg. Chim. Acta*, 1985, **105**, 89.
23 M. Arunchaiya, J. H. Morris, S. J. Andrews, D. A. Welch, and A. J. Welch, *J. Chem. Soc. Dalton Trans.*, 1984, 2525.
24 C. E. Nordman and C. Reimann, *J. Am. Chem. Soc.*, 1959, **81**, 3538.
25 S. J. Andrews and A. J. Welch, *Inorg. Chim. Acta*, 1984, **88**, 153.
26 S. J. Andrews and A. J. Welch, *Acta Crystallogr., Sect. C*, 1985, **41**, 1496.
27 L. D. Brown and W. N. Lipscomb, *Inorg. Chem.*, 1977, **16**, 1.
28 C. J. Fritchie, *Inorg. Chem.*, 1967, **6**, 1199.
29 M. R. Churchill, in 'Transition Metal Hydrides,' ed. R. Bau, Adv. Chem. Ser., American Chemical Society, 1978, vol. 167, pp. 38—39.
30 M. R. Churchill, P. H. Bird, H. D. Kaesz, R. Bau, and B. Fontal, *J. Am. Chem. Soc.*, 1968, **90**, 7135.
31 B. F. G. Johnson, J. Lewis, P. R. Raithby, G. M. Sheldrick, and G. Suss, *J. Organomet. Chem.*, 1978, **162**, 179.
32 D. M. P. Mingos, *J. Chem. Soc., Dalton Trans.*, 1977, 602.
33 E. A. McNeill, K. L. Gallaher, F. R. Scholer, and S. H. Bauer, *Inorg. Chem.*, 1973, **12**, 2108.
34 M. J. S. Dewar and M. L. McKee, *J. Am. Chem. Soc.*, 1977, **99**, 5231.
35 M. J. S. Dewar and M. L. McKee, *Inorg. Chem.*, 1978, **17**, 1569.
36 M. J. S. Dewar and M. L. McKee, *Inorg. Chem.*, 1980, **19**, 2662.
37 A. J. Schultz, J. M. Williams, R. B. Calvert, J. R. Shapley, and G. D. Stucky, *Inorg. Chem.*, 1979, **18**, 319.
38 M. McPartlin, C. R. Eady, B. F. G. Johnson, and J. Lewis, *J. Chem. Soc., Chem. Commun.*, 1976, 883.

Received 23rd June 1986; Paper 6/1258